

## Dynamics of the Solid and Liquid Phases in Dilute Sheared Brownian Suspensions: Irreversibility and Particle Migration

Jennifer R. Brown,<sup>1</sup> Joseph D. Seymour,<sup>1,\*</sup> Sarah L. Codd,<sup>2</sup> Einar O. Fridjonsson,<sup>1</sup> Giles R. Cokelet,<sup>1</sup> and Magnus Nydén<sup>3</sup>

<sup>1</sup>Department of Chemical and Biological Engineering, Montana State University, Bozeman, Montana 59717-3920 USA

<sup>2</sup>Department of Mechanical and Industrial Engineering, Montana State University, Bozeman, Montana 59717-3920 USA

<sup>3</sup>Department of Chemical and Biological Engineering, Chalmers University of Technology, SE-412 96 Göteborg, Sweden

(Received 23 July 2007; published 11 December 2007)

Magnetic resonance measurements of migration and irreversible dynamics in the capillary shear flow of a Brownian suspension are presented. The results demonstrate the presence of phenomena typically associated with concentrated noncolloidal systems and indicate the role of many body hydrodynamics in dilute Brownian suspension transport. The application of concepts from chaos theory and nonequilibrium statistical mechanics is demonstrated.

DOI: 10.1103/PhysRevLett.99.240602

PACS numbers: 05.70.Ln, 47.57.J-, 47.61.Ne, 82.70.Dd

Transport of colloidal suspensions under shear forces plays an elemental role in industry and biology. The dynamics of cellular bacteria in microbiology [1], red blood cells in physiology [2], and colloidal contaminants in earth formations [3] impact the system function and transport. Understanding colloidal dynamics is also required for design of products such as drug delivery agents and microfluidic devices [4]. Brownian suspensions have been the subject of many experimental and numerical studies [5]. Experimental studies have primarily tracked the particle phase and to our knowledge no noninvasive direct simultaneous measurements of both the discrete particle and continuous liquid phase dynamics under shear have been reported. We apply pulsed gradient spin echo (PGSE) nuclear magnetic resonance (NMR) methods to directly measure the propagator of the motion [6] and diffusivity [7] of each phase by spectral resolution [8,9], in dilute hard sphere suspensions undergoing shear flow in a capillary. Recent optical experiments and theory for colloidal particles in shear flow indicate the presence of particle migration [10], an effect thought to occur only in noncolloidal suspensions. Additionally experiments and simulations for concentrated noncolloidal suspensions in shear flow have indicated chaotic particle dynamics leading to irreversibility [11]. The data presented here indicate the presence of both particle migration and irreversibility in dilute, volume fraction  $\phi < 0.10$ , Brownian suspensions. These results indicate that modeling of the transport and mixing due to particle dynamics in sheared dilute colloidal suspensions can benefit from adoption of tools from chaos theory and nonequilibrium statistical mechanics [12].

Core shell oil filled particles [13] suspended in water allow measurement of the particle and liquid phase dynamics using NMR spectral resolution [8]. The uncharged polymer shell confers hard sphere behavior to the particles [14]. PGSE NMR has been previously applied to measure the oil diffusion within the particle and the particle Brownian diffusivity for  $1.51 \mu\text{m}$  radius spheres as a function of particle concentration [15] and the nanometer

scale particle phase velocity in Couette flow of concentrated ( $\phi = 0.46$ )  $185 \text{ nm}$  radius spheres [14]. In this work, the core shell particle and suspending water dynamics for shear flow of dilute ( $\phi < 0.10$ )  $a = 1.25 \pm 0.46 \mu\text{m}$  radius spheres in a  $R = 500 \mu\text{m}$  radius capillary are resolved independently by enhancing water  $T_1$  spin-lattice magnetic relaxation to allow spectral resolution between oil within the spheres and suspending water. The bulk velocity in the capillary is imaged for a dilute suspension of  $\phi = 0.08$  using PGSE NMR imaging of all the protons providing the composite axial velocity of the oil and water [9], and is shown in Fig. 1 to be nearly the parabolic velocity profile of laminar Poiseuille flow for a Newtonian fluid. The particle size based Reynolds and Peclet numbers are  $\text{Re}_p = \rho_f a^2 \langle \dot{\gamma} \rangle / \mu_f = 5.7$ ,  $\text{Pe}_p = a^2 \langle \dot{\gamma} \rangle / D_{SE} = 39$ .  $\text{Re}$  is the ratio of inertial to viscous forces while  $\text{Pe}$  indicates the rate ratio of advective to diffusive mass transfer, indicating the experiments are in the low inertia advective transport regime.

Using spectrally resolved PGSE, the propagator  $P(Z, \Delta)$ , or probability distribution of displacements  $Z$  over a time  $\Delta$ , of the oil in the particles and the suspending

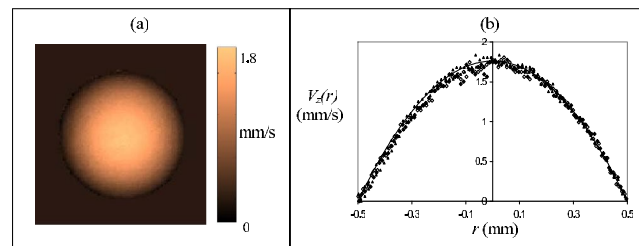


FIG. 1 (color online). Composite axial velocity for  $\phi = 0.08$  suspension flow in 1 mm capillary, average velocity of  $0.88 \text{ mm/s}$  ( $\text{Re}_{\text{tube}} = 0.88$ ,  $\text{Re}_p = 5.7$ ). (a) Image of spatial distribution of velocity in plane perpendicular to flow,  $14 \times 14 \mu\text{m}$  resolution. (b) Velocity as function of radius across various diameters (symbols) and the parabolic velocity profile  $V_z(r) = V_{\text{max}}(1 - r^2/R^2)$  for Poiseuille flow (black line).

water are obtained. The dynamics of each phase are thus individually resolved as shown in Fig. 2. The propagator is displayed as a probability distribution of axial velocities  $v_z = Z/\Delta$  for a single displacement time  $\Delta = 30$  ms. The normalized spin echo signal is  $E(q, \Delta) = \int P(Z, \Delta) \times \exp(i2\pi qZ) dZ$ , and full displacement space is sampled through the reciprocal wavenumber to displacement  $q = (2\pi)^{-1} \gamma_m g \delta$ , which depends on the nuclei gyromagnetic ratio,  $\gamma_m$  and pulsed magnetic field gradient amplitude  $g$  (0 to 1.78 T/m) and duration  $\delta$  (3.5 ms). The propagators are normalized to the total signal of the respective oil or water phase. The velocity probability distribution for pure water flow in the 500  $\mu\text{m}$  capillary is the hat function for the parabolic spatial velocity distribution of pure water, indicating equal probabilities of velocity from 0 to  $v_{\text{max}}$ , convolved with the Gaussian for water diffusion [16]. The displacement observation time is short enough that

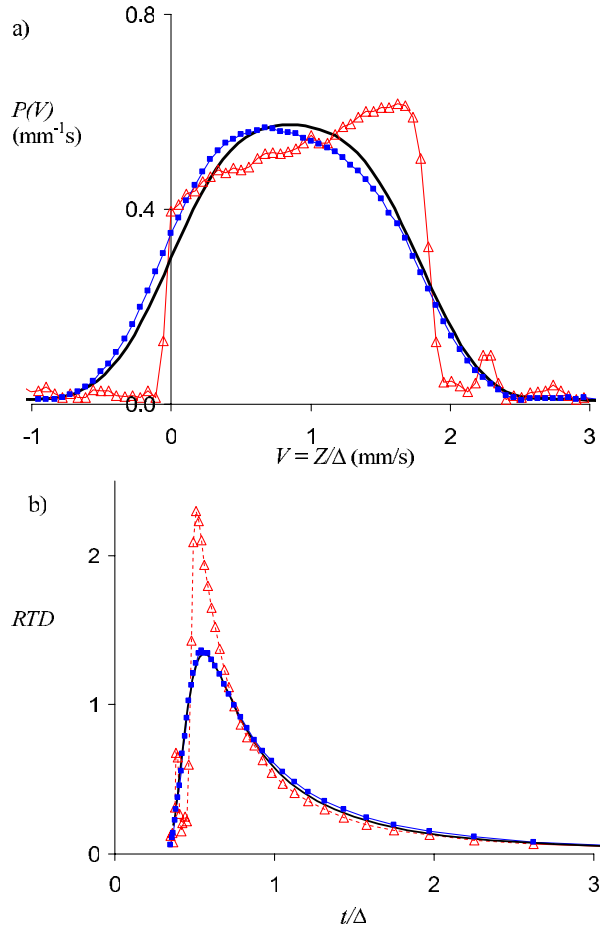


FIG. 2 (color online). (a) Propagators for water (black line) and  $\phi = 0.08$  suspension (blue closed squares suspending water, red open triangles core oil particles) flowing at  $V_{\text{ave}} = 0.88$  mm/s ( $Re_p = 5.7$ ,  $Pe_p = 39$ ) over an observation time  $\Delta = 30$  ms. The order of magnitude differences in  $D_w$  and  $D_{SE}$  gives the particle propagator sharper edges. (b) Corresponding residence time distributions.

Taylor dispersion [17] does not impact the fluid,  $\Delta \ll R^2/D_w \sim 10^4$  s, or the particles,  $\Delta \ll R^2/D_{SE} \sim 10^6$  s, where the water diffusivity is  $D_w = 1.9 \times 10^{-9}$   $\text{m}^2/\text{s}$  and the Stokes-Einstein particle diffusivity is  $D_{SE} = kT/6\pi\mu_f a = 1.76 \times 10^{-13}$   $\text{m}^2/\text{s}$ . Comparing the water propagator for the pure fluid flow and the suspending fluid in the Brownian suspension flow, the dynamics are clearly different with the suspending fluid skewed toward lower velocities. The particle dynamics are biased toward the fastest velocities, a direct consequence of particle migration to the faster streamlines, shown in Fig. 1 to be near the tube center.

In averaged transport theory for two-phase flow, derived from ensemble or volume averaging of the equations of motion, additional stress generation terms due to velocity fluctuations in the fluid  $\mathbf{v}_f' = \mathbf{v}_f - \langle \mathbf{v}_f \rangle$  and particle  $\mathbf{v}_p' = \mathbf{v}_p - \langle \mathbf{v}_p \rangle$  phases and differences between the averages  $\langle \mathbf{v}_f \rangle - \langle \mathbf{v}_p \rangle$  arise [18]. These terms are of the form of Reynolds stresses generated by velocity fluctuations in turbulent flow [18]. The velocity measured in the PGSE experiment is averaged over time, space and ensembles of the flow. Each experimental signal acquisition is encoded for displacement  $1/q$  over time  $\Delta = 30$  ms and the signals are averaged 8 times. Since flow causes spins whose dynamics were probed during an acquisition to vacate the coil region, a new ensemble is probed during each subsequent acquisition. The flow is steady but exact initial particle phase configurations vary. The displacement encoding magnetic field gradient is incremented 128 times to sample the entire reciprocal space to displacement. Fourier transform in  $q$  results in a propagator averaged over the entire experiment time ( $\sim 1$  hour), the capillary volume within the NMR coil and the ensembles of particle configurations. The coincidence of the propagators for the solid particles and suspending fluid on the axial velocity abscissa demonstrates the particles and fluid have the same velocity range but the overall average particle and fluid velocities are different. The propagators characterize system transport and mixing in terms of the residence time distributions (RTD's) [19–21], as shown in Fig. 2(b). The scale dependent RTD's depend on the experimental displacement encoding time and the average velocity, as if the tube length were varied [21]. The impact of the particle migration causes a significant variation in the residence time of each phase within the system, even in dilute suspensions.

Measurement of scale dependent diffusion by PGSE NMR has found broad application ranging from polymer dynamics [22] to hydrodynamic dispersion [16,23] and granular dynamics [24]. The nonequilibrium time dependent Green-Kubo relation for the diffusion coefficient in the  $i$  direction is obtained in the long wavelength hydrodynamic limit  $q \rightarrow 0$  for diffusivity of the  $m = s, f$  phase as  $D_{ii,m}^*(\Delta) = \int_0^\Delta \langle v_{i,m}'(\tau) v_{i,m}'(0) \rangle d\tau$  [12,25]. The measured effective diffusivity characterizes the velocity fluctuations of each phase in the direction  $i$  of the

applied magnetic field gradient. Figure 3 shows the effective axial diffusion for the solid  $D_{zz,s}^*(\Delta)$  and fluid  $D_{zz,f}^*(\Delta)$  at an observation time of  $\Delta = 100$  ms, scaling as a function of the average shear rate. The impact of Taylor dispersion on the oil particles due to diffusion across streamlines [17] is minimal in this data since the radial diffusion of  $0.2 \mu\text{m}$  causes a velocity variation of less than  $0.4 \mu\text{m/s}$  during the 100 ms observation time.

Dilute Brownian hard sphere suspensions are often treated as reversible systems, in analogy with dilute gases in kinetic theory, accounting only for two body interactions. PGSE NMR is able to compensate for motions that are reversible over the displacement measurement time scale  $\Delta$  [9,16,24–26]. Repetition of the motion encoding magnetic field gradients with reverse polarity of the second pulse pair results in reversal of the coherent spin magnetization phase shift generated due to affine displacements which are non fluctuating, or coherent, in each interval  $\Delta$ . Figure 4 shows the particle phase effective diffusion coefficient measured as a function of displacement observation time by flow compensated PGSE. The open symbols are effective diffusion of the oil in the particles in the axial (circles)  $D_{zz,s}^*(\Delta)$  and transverse (triangles)  $D_{yy,s}^*(\Delta)$  directions in the absence of shear flow. The diffusion coefficients decrease with increasing displacement time due to the dominant effect of the restricted motion of the oil within the particle convolved with the Stokes-Einstein particle scale diffusion [15]. Upon imposition of shear flow the transverse diffusion (closed triangles), which is a composite of the diffusivity in the vorticity ( $\theta$ ) and shear ( $r$ ) directions, exhibits the same behavior as in the absence of shear over the time range sampled. In contrast, under

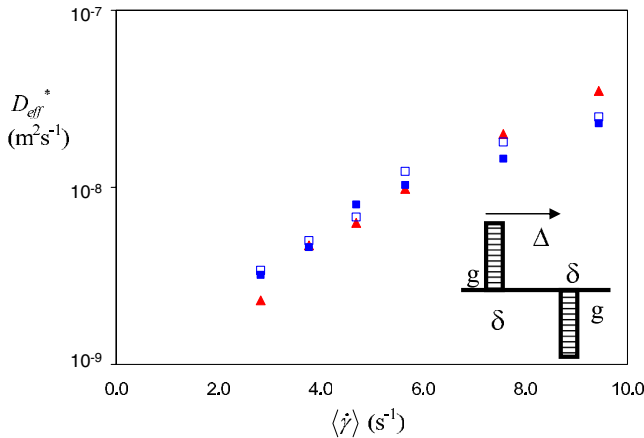


FIG. 3 (color online). Effective diffusion  $D_{\text{eff}}^*$  as a function of average shear rate  $\langle \dot{\gamma} \rangle = -\frac{4\langle v_z \rangle}{3R} \propto \text{Pe}$ , during flow of  $\phi = 0.08$  suspension for the suspending water  $D_{zz,f}^*$  (blue closed squares) and particles  $D_{zz,s}^*$  (red open triangles), as well as pure water flow  $D_{zz}^*$  (blue open squares) measured using single PGSE (inset) which is sensitive to the distribution of reversible velocities, for displacement time  $\Delta = 100$  ms.

shear flow the axial diffusivity exhibits a noisy decrease due to variability in the reversibility of the dynamics, followed by a transition to an increasing function of time, or total strain as shown in Fig. 4(b). This indicates that after a displacement time of 100 ms shear induced particle dynamics are no longer reversible and nonequilibrium time dependent dynamics govern transport in dilute Brownian suspensions.

The onset of irreversible particle dynamics in concentrated noncolloidal suspensions has been attributed to nonlinear many body hydrodynamic interactions through experiment and simulation [11]. The velocity of particle  $j$  is approximated as the sum of passive advection at the location of the particle and the velocity distribution due to the  $N$  particles,  $\dot{\mathbf{r}}_j = a\dot{\gamma}_j + a^2\dot{\gamma}_j \sum_{j \neq k}^N \mathbf{U}(\mathbf{r}_k - \mathbf{r}_j)$ . The particle interaction velocities are given by the summation of the Oseen Tensor, or Green's function for a point force

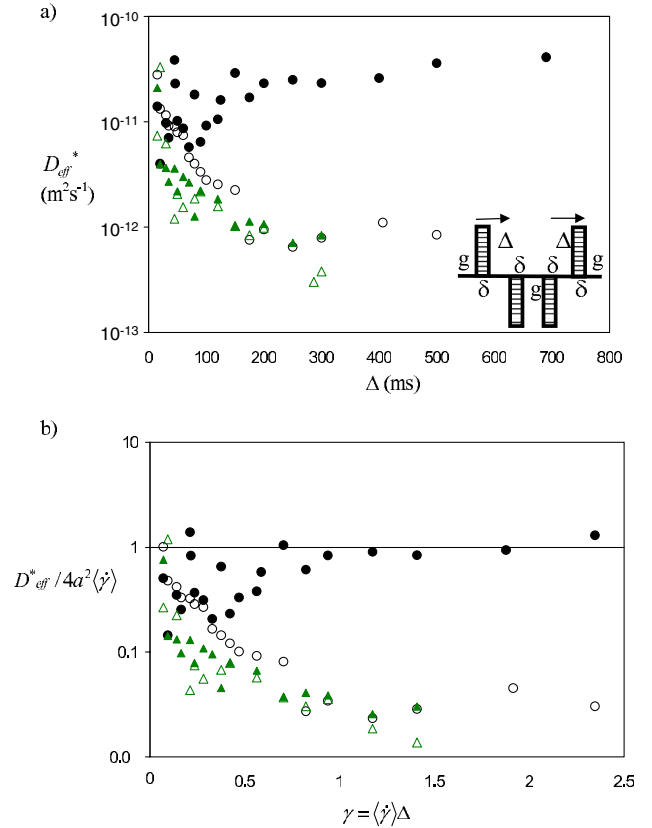


FIG. 4 (color online).  $D_{\text{eff}}^*$   $\phi = 0.08$  suspension obtained using flow compensated PGSE sequence (inset in (a)), which measures only irreversible stochastic motions. (a) For an average velocity of  $0.88 \text{ mm/s}$  ( $\text{Re}_p = 5.7$ ,  $\text{Pe}_p = 39$ )  $D_{\text{eff}}^*$  for the particle core oil as a function of observation time  $\Delta$  in the flow direction  $z$ ,  $D_{zz,s}^*$  (black closed circles), in the velocity gradient direction  $y$ ,  $D_{yy,s}^*$  (green closed triangles), and in the absence of flow in the  $z$ ,  $D_{zz,s}^*$  (black open circles) and  $y$ ,  $D_{yy,s}^*$  (green open triangles) directions. (b)  $D_{\text{eff}}^*$  normalized by the average shear rate  $\langle \dot{\gamma} \rangle$  and the square of the particle diameter  $4a^2$  as a function of accumulated strain  $\gamma = \langle \dot{\gamma} \rangle \Delta$ .

in the Stokes equations, and for  $N \geq 3$  chaotic scattering of the velocity fields is present [27]. Particle properties that can impact reversibility are roughness and size. The core shell particles are smooth, as indicated by scanning electron microscopy, and are in the size range for which Taylor dispersion due to Brownian motion are negligible on the experimental time scale. This along with the scaling of the particle effective diffusion as predicted for shear induced diffusivity [5],  $D_{zz,s}^* \sim a^2 \langle \dot{\gamma} \rangle$ , indicates that three body hydrodynamic interactions or chaotic scattering events [27] are responsible for the irreversible dynamics in Fig. 4. The increase in the diffusion with increasing accumulated strain or time is associated with the exponential spreading of particle trajectories, an effect characterized by a positive Lyapunov exponent [11,27]. A current topic of research interest is establishing the exact form of transport coefficients based on time correlation functions from dynamical systems theory models of microscale dynamics [12,28]. This has been done for scattering systems, such as the Lorentz gas, using the escape rate formalism leading to definition of the diffusion in terms of the sum of the positive Lyapunov exponents  $\lambda_j$  and the Kolmogorov-Sinai entropy  $h_{KS}$ ,  $D = \lim_{l \rightarrow \infty} \frac{l^2}{\pi^2} (\sum_{\lambda_j > 0} \lambda_j - h_{KS})$  [12,28]. As demonstrated here, dilute colloidal systems present an experimentally accessible model to further study the relationship between chaotic dynamics and transport coefficients.

The data presented indicate that particle interactions which generate irreversible non equilibrium dynamics and particle migration are important in dilute Brownian suspensions composed of particles of a size relevant to the transport of microbes [1], contaminants [3] and blood cells [2]. As in reference [11] our experiments exhibit a transition from reversible to irreversible dynamics dependent on the accumulated shear strain applied to the suspension. The order of magnitude and timescale of the diffusive dynamics indicates shear induced hydrodynamic interactions are responsible. The observation of strain induced irreversible dynamics in dilute Brownian suspensions indicates the applicability of chaotic dynamics and non equilibrium statistical mechanics methods to model these systems.

Research support by NSF No. CTS-0348076 (J.D.S.), No. CBET-0642328 (S.L.C.), and NIH No. P20 RR-

16455-04 (J.R.B.).

\*jseymour@coe.montana.edu

- [1] T. Fenchel, *Science* **296**, 1068 (2002).
- [2] H.L. Goldsmith, G.R. Cokelet, and P. Gaetgens, *Am. J. Physiol.* **257**, H1005 (1989).
- [3] A.B. Kersting *et al.*, *Nature (London)* **397**, 56 (1999).
- [4] H.A. Stone and S. Kim, *AIChE J.* **47**, 1250 (2001).
- [5] J.F. Brady, *Curr. Opin. Colloid Interface Sci.* **1**, 472 (1996).
- [6] L. Van Hove, *Phys. Rev.* **95**, 249 (1954).
- [7] E.O. Stejskal and J.E. Tanner, *J. Chem. Phys.* **42**, 288 (1965).
- [8] P. Stilbs, *Prog. Nucl. Magn. Reson. Spectrosc.* **19**, 1 (1987).
- [9] P.T. Callaghan, *Principles of Nuclear Magnetic Resonance Microscopy* (Oxford University, New York, 1991).
- [10] M. Frank *et al.*, *J. Fluid Mech.* **493**, 363 (2003).
- [11] D.J. Pine *et al.*, *Nature (London)* **438**, 997 (2005).
- [12] J.R. Dorfman, *An Introduction to Chaos in Nonequilibrium Statistical Mechanics* (Cambridge University, Cambridge, England, 1999), Vol. 14.
- [13] A. Loxley and B. Vincent, *J. Colloid Interface Sci.* **208**, 49 (1998).
- [14] H. Wassenius and P.T. Callaghan, *J. Magn. Reson.* **169**, 250 (2004).
- [15] H. Wassenius, M. Nyden, and B. Vincent, *J. Colloid Interface Sci.* **264**, 538 (2003).
- [16] S.L. Codd *et al.*, *Phys. Rev. E* **60**, R3491 (1999).
- [17] G.I. Taylor, *Proc. R. Soc. A* **219**, 186 (1953).
- [18] D.A. Drew, *Physica (Amsterdam)* **179A**, 69 (1991).
- [19] P.V. Danckwerts, *Chem. Eng. Sci.* **2**, 1 (1953).
- [20] I. Mezic, S. Wiggins, and D. Betz, *Chaos* **9**, 173 (1999).
- [21] S.L. Codd *et al.*, in *NMR Imaging in Chemical Engineering*, edited by S. Stapf and S.-I. Han (Wiley, USA, 2006).
- [22] E. Fischer *et al.*, *Phys. Rev. E* **62**, 775 (2000).
- [23] A. Ding and D. Candela, *Phys. Rev. E* **54**, 656 (1996).
- [24] J.D. Seymour *et al.*, *Phys. Rev. Lett.* **84**, 266 (2000).
- [25] P.T. Callaghan, S.L. Codd, and J.D. Seymour, *Concepts Magn. Reson.* **11**, 181 (1999).
- [26] A.A. Khrapitchev and P.T. Callaghan, *Phys. Fluids* **15**, 2649 (2003).
- [27] I.M. Janosi *et al.*, *Phys. Rev. E* **56**, 2858 (1997).
- [28] P. Gaspard, *Int. J. Mod. Phys. B* **15**, 209 (2001).